

Analysis of the absorption spectra and spectral hole burning in zero-phonon lines of F_3^+ and N_1 colour centres in LiF crystals

A.V. Fedorov, D.V. Martyshkin, V.V. Fedorov

Abstract. The temperature dependences and mechanisms of broadening of zero-phonon lines of F_3^+ (488 nm) and N_1 (523 nm) colour centres in LiF crystals are investigated. The results obtained make it possible to determine the quadratic electronic–vibrational coupling constant for N_1 colour centres. The experimental data on the spectral hole burning in zero-phonon lines of F_3^+ and N_1 colour centres indicate that the latter are positively charged.

Keywords: spectral hole burning, zero-phonon lines, colour centres.

1. Introduction

Spectral hole burning is one of the most important spectroscopic methods for studying the properties of optical centres in solids. It is also used to stabilise single-frequency lasers and record high-density optical data. The latter possibility can be very urgent in designing quantum computers [1–4]. Although LiF crystals with colour centres (CCs) belong to the most widely spread CC-containing crystals applied in quantum electronics (in particular, as passive Q switches and active laser media) [5–7], only few studies were devoted to hole burning in their spectra.

In this field, among the first were Moerner et al. [8], who described and analysed for the first time the spectral hole burning in absorption zero-phonon lines (ZPLs) of F_3^+ CCs in pure and doped LiF crystals. Hole burning in spectra of the F_2^- CCs of LiF crystal was reported for the first time in [9]. The spectral hole in the absorption ZPL had existed for two weeks under room temperature storage, although the hole could be observed only at a liquid-helium temperature. Kazumata [10] reported hole burning in a ZPL at the wavelength $\lambda = 601$ nm and assigned it to F_2 CCs. However, the ZPL at $\lambda = 601$ nm is far from the overlap range of the absorption and luminescence bands of F_2 CCs [11]. In addition, the ZPL at $\lambda = 601$ nm is observed not in all irradiated crystals with F_2 CC; therefore, it should be rather assigned to a complex aggregate of centres. Further studies are necessary to identify this ZPL more precisely.

The ZPL of F_3^+ CCs was identified in [12–14]. It was shown there that the F_3^+ centre can be considered as a combination of two electrons in an equilateral triangle, whose vertices are neighboring anion vacancies in the LiF lattice. The spatial symmetry of this centre was analysed for the first time by Feofilov [12], and this investigation was continued by Bauman et al. [13]. This system has a C_{3v} point symmetry. The identification of the N_1 -CC ZPL is less definite. In [15, 16] it was attributed to F_4 CC, whereas in [17] it was assigned to the isomer F_3^* CC. The symmetry of this CC was studied using piezospectroscopy and Stark effect in [18, 19]. It was shown that the N_1 centre has the C_{2h} symmetry and is either shaped as a rhombus composed of four F centres or is an aggregate state composed of two F centres with a (112) axis.

The CC ionisation rate under laser irradiation depends strongly on the CC charge. The spectral hole burning rate in the ZPL of positively charged CC should be much lower than in the ZPLs of neutral and negatively charged CCs. Thus, the comparison of the experimental data on hole burning in the N_1 -, F_3^+ -, and F_3^* -CC spectra allowed us to determine the charge state of the N_1 CC.

In this paper, we report the results of spectroscopic study of the ZPLs of F_3^+ (488 nm) and N_1 (523 nm) CCs in LiF crystals. We investigated the possibility of spectral hole burning in these lines under high-power nanosecond resonant laser excitation at low temperatures. In addition, the temperature broadening of these ZPLs was analysed within the theory of electron–phonon coupling, which was developed nonperturbatively in [20, 21].

2. Experimental

Samples of crystals were placed in a closed-cycle cryostat (Model CCS 450, Janis Research), which allowed for sample cooling down to 14 K. The sample temperature was measured using a temperature controller (Autotuning Temperature Controller Model 330, Lake Shore) with a silicon diode as a temperature sensor. The low-temperature luminescence and absorption spectra were measured with an ARC-750 spectrometer (Acton Research), connected to a computer. The spectral resolution of the spectrometer was 0.5 cm^{-1} . The signals from the optical detector (FEU) were recorded using a lock-in amplifier (Model 7265, EG&G Instruments) when measuring the absorption spectrum and a boxcar integrator (SR250, Standard Research Systems) when measuring the spectra of laser pulses. The laser source was an optical parametric oscillator (Quanta-Ray MOPO-SL, Spectra Physics) with the following typical character-

A.V. Fedorov Moscow Institute of Physics and Technology (State University), Institutskii per. 9, 141700 Dolgoprudnyi, Moscow region, Russia; e-mail: tohach@gmail.com;

D.V. Martyshkin, V.V. Fedorov University of Alabama at Birmingham, USA, 1600, University blvd.

Received 26 April 2010

Kvantovaya Elektronika 40 (7) 647–651 (2010)

Translated by Yu.P. Sin'kov

istics: signal wave tuning range of 440–690 nm and idler wave tuning range of 735–1800 nm. The spectral linewidth was less than 0.2 cm^{-1} at a pulse duration of 6 ns and the pulse repetition rate of 10 Hz. To form CCs in LiF crystals, the latter were γ -irradiated (dose 10^8 rad , ^{60}Co source) at room temperature ($T = 300 \text{ K}$). The irradiated crystals were kept at room temperature for more than seven years.

3. Results and discussion

The experimental wavelength dependences of the absorption coefficient of F_3^+ CCs are shown in Fig. 1a. The temperature dependence of the ZPL width at $\lambda = 487.5 \text{ nm}$ is presented in Fig. 1b. One can see in Fig. 1a that, along with the ZPL at $\lambda = 487.5 \text{ nm}$, there is a one-phonon transition at $\lambda = 482.6 \text{ nm}$, which corresponds to the effective phonon vibration frequency $\nu = 203 \text{ cm}^{-1}$. No change in the ZPL position with a change in temperature was found within the experimental error. The ZPL FWHM $\Delta\nu$ was 15 cm^{-1} at low temperatures. The linewidth significantly changed at temperatures $T > 30 \text{ K}$. The spectral FWHM $\Delta\nu_{\text{1ph}}$ of the one-phonon peak at $\lambda = 482.6 \text{ nm}$ was 43 cm^{-1} at $T = 14 \text{ K}$.

Similar measurements were performed for the N_1 centre with a ZPL at $\lambda = 523.4 \text{ nm}$ (Fig. 2). The effective phonon frequency $\nu = 209 \text{ cm}^{-1}$ for this centre was determined from the absorption spectrum at $T = 16 \text{ K}$. The peak of the ZPL at $\lambda = 523.4 \text{ nm}$ becomes red-shifted with increasing temperature (Fig. 2a). We performed several successive

measurements of the transmission spectrum of the crystal to make sure that the ZPL shift is not due to the systematic error of the spectrometer. The first measurements were performed at a low temperature ($T = 16 \text{ K}$); then the crystal was heated to $T = 100 \text{ K}$; and, finally, cooled to $T = 16 \text{ K}$. The initial and final spectra completely coincided. One can see in Fig. 2b that the ZPL width at low temperatures is 11 cm^{-1} and increases with temperature up to $\sim 70 \text{ K}$, in contrast to the ZPL width for F_3^+ CC ($\sim 45 \text{ K}$). The spectral FWHM of the one-phonon peak at $\lambda = 517.7 \text{ nm}$ and $T = 14 \text{ K}$ is $\sim 55 \text{ cm}^{-1}$.

The temperature dependence of the ZPL behaviour was analysed using the dynamic theory, which takes into account the quadratic electron–phonon coupling. This theory was nonperturbatively developed in [20, 21]. When this coupling is related to acoustic lattice vibrations, the temperature shift $\delta\nu$ and ZPL width $\Delta\nu$ are determined by the equations [19]

$$\delta\nu = \nu_D \frac{3}{2} \left(\frac{W}{1+W} \right) \left(\frac{T}{T_D} \right)^4 \int_0^{T_D/T} dx \frac{x^3}{e^x - 1}, \quad (1)$$

$$\Delta\nu = \nu_D \frac{9\pi}{2} \left(\frac{W}{1+W} \right) \left(\frac{T}{T_D} \right)^7 \int_0^{T_D/T} dx \frac{x^6 e^x}{e^x - 1}, \quad (2)$$

where T_D and ν_D are, respectively, the Debye temperature and Debye frequency ($h\nu_D = k_B T_D$); and W is the dimensionless quadratic-coupling constant. The Debye temperature for the LiF crystal is $\sim 730 \text{ K}$ [22]. At low

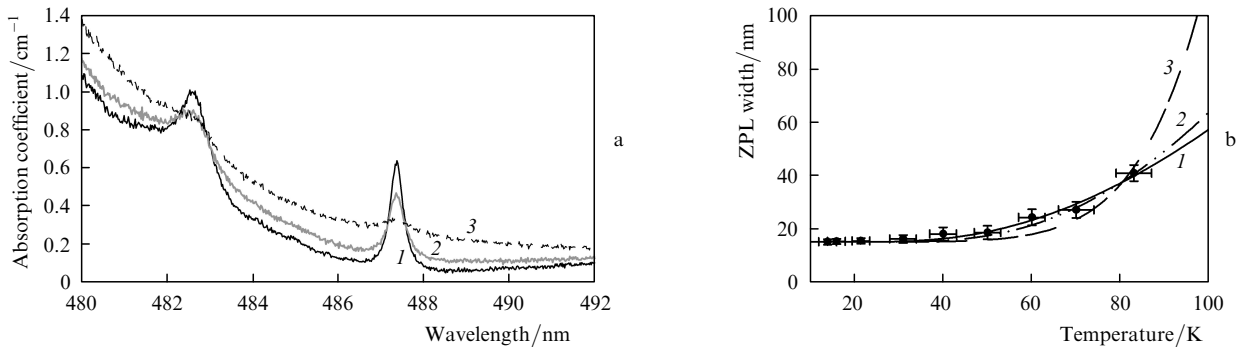


Figure 1. (a) Experimental absorption spectra at $T = (1) 16, (2) 50,$ and $(3) 83 \text{ K}$ and (b) the calculated (curves) and experimental (circles) temperature dependences of the ZPL width at $\lambda = 487.5 \text{ nm}$; the calculation was performed taking into account the CC coupling with (1) a local vibration, (2) a local vibration at a fixed frequency, and (3) acoustic vibrations.

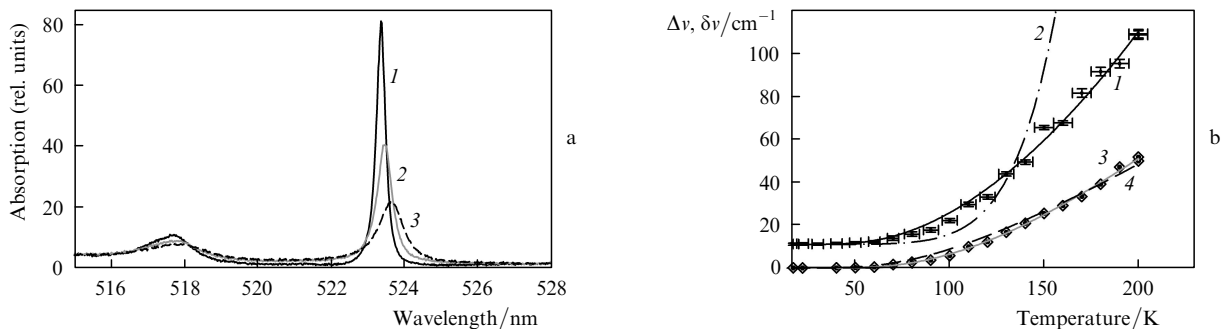


Figure 2. (a) Experimental absorption spectra at $T = (1) 17, (2) 90,$ and $(3) 110 \text{ K}$ at and (b) calculated (curves) and experimental (symbols) temperature dependences of the (1, 2) width $\Delta\nu$ and (3, 4) shift $\delta\nu$ of the ZPL peak at $\lambda = 523.4 \text{ nm}$; the calculation was performed (1, 2) taking into account the CC coupling with (1) a quasi-local vibration and (2) acoustic vibrations, (3) at a fixed phonon frequency, and (4) with free parameters ν_0 and W .

temperatures ($T \ll T_D$) expressions (1) and (2) are transformed into the relations $\delta\nu \sim (T/T_D)^4$ and $\Delta\nu \sim (T/T_D)^7$.

In the other case the quadratic electron–phonon coupling is due to the local optical phonon, and the corresponding expression for the ZPL temperature shift and broadening take the form [23]

$$\delta\nu = \pi W v_0 n(\nu_0, T), \quad (3)$$

$$\Delta\nu = \frac{\pi}{2} W^2 v_0^2 \tau n(\nu_0, T) [n(\nu_0, T) + 1], \quad (4)$$

where ν_0 is the local-mode frequency; τ is the phonon state lifetime; and $n(\nu_0, T) = \{\exp[h\nu_0/(k_B T)] - 1\}^{-1}$ is the Bose factor. In this study the temperature dependences of the spectra of F_3^+ - and N_1 -CC ZPLs were analysed using both approximations. The temperature dependences of the experimental results were described taking into account the ZPL inhomogeneous broadening (Δ_{inh}), obtained by measuring spectra at $T = 14$ K.

Based on the method of least squares, the dependence of the ZPL spectral width at $\lambda = 487.5$ nm in the temperature range of 14–84 K is best described in terms of coupling between CC and a local vibration mode with $\nu_0 = 150$ cm^{-1} and $\frac{1}{2}\pi W^2 v_0^2 \tau = 282$ cm^{-1} [Fig. 1b, curve (1)]. It can be seen that the obtained quasi-local vibration frequency is somewhat below the value determined from the absorption spectrum ($\nu_0 = 203$ cm^{-1}). However, the curve with the fixed effective frequency $\nu = 203$ cm^{-1} also describes (within the experimental error) the ZPL temperature broadening at $\lambda = 487.5$ nm with the constant $\frac{1}{2}\pi W^2 v_0^2 \tau = 810$ cm^{-1} [Fig. 1b, curve (2)]. The calculation based on the theory taking into account the CC coupling with acoustic lattice vibrations gives a significant deviation from the experimental data [Fig. 1b, curve (3)].

The temperature dependence of the width of ZPL at $\lambda = 523$ nm is shown in Fig. 2b. The attempt to describe the experimentally obtained ZPL width in correspondence with the theory taking into account CC coupling with acoustic lattice vibrations is no success [Fig. 2b, curve (2)]; at the same time the ZPL broadening due to the CC coupling with a quasi-local vibration is in good agreement with the experimental data. Curve (1) in Fig. 2b was plotted according to Eqn (4) with the following parameters: the

quasi-local vibration frequency $\nu_0 = 209$ cm^{-1} and the coefficient $\frac{1}{2}\pi W^2 v_0^2 \tau = 270$ cm^{-1} .

For further analysis it is convenient to introduce a dimensionless constant $W^2 v_0 \tau$. It determines the slope of the temperature dependence and, therefore, in the first-order approximation it is the same as in the approximation of experimental points by Eqn (4) with different quasi-local vibration frequencies. In our case $W^2 v_0 \tau = 0.82$. As was noted above, the experiments revealed the change in the ZPL peak position with temperature. Our measurements make it possible to directly obtain the quadratic-change constant (whereas the equation for temperature broadening contains, along with this constant, the quasi-local vibration lifetime).

The temperature dependence of the ZPL shift was analysed under two assumptions. In the first one, the local phonon frequency and nonlinear coupling constant were considered as free parameters. In this case, the method of least squares gives the following results: $\nu_0 = 268$ cm^{-1} and $W = 0.36$ [Fig. 2b, curve (4)]. In the second one, where the phonon frequency ν_0 was assumed to be 209 cm^{-1} , the coupling constant $W = 0.26$ [Fig. 2b, curve (3)]. The value of this coupling constant allows one to estimate the product $\nu_0 \tau$, which turned out to be $\sim 6 - 12$ (for $W \approx 0.26 - 0.36$).

In further experiments we studied the ZPL absorption spectra as functions of the laser irradiation time. The spectral hole burning was performed by radiation of optical parametric oscillator with an average power of 1–10 mW and a pulse repetition rate of 10 Hz, which was focused into a spot 1.5 mm in diameter on the sample surface at a temperature of 14 K. The wavelength dependences of the optical crystal density, obtained under laser irradiation near the N_1 -CC band are shown in Fig. 3. The ZPL optical density significantly changed (by a factor of 2.3) during the first 25 s of irradiation. Then the change rate considerably decreased, and the optical density decreased from 1.78 to 1.17 for the next 165 s. The change in the absorption spectrum was accompanied by both a nonselective change in absorption throughout the entire ZPL width and an additional selective change in absorption near the laser wavelength. Figure 3 shows for comparison the laser radiation spectrum measured on the same spectrometer [curve (1)]. One can see that the laser radiation line is significantly overlapped with the CC ZPL and only slightly shifted to the longer wavelengths with respect to the

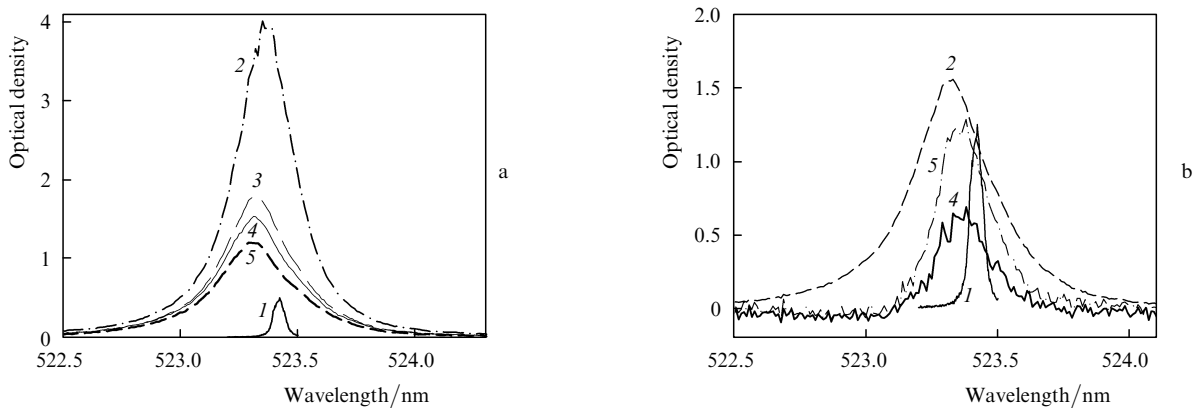


Figure 3. Spectral hole burning in the ZPL at $\lambda = 523.4$ nm: (1) the laser radiation spectrum; (2) the absorption spectrum before irradiation; and (a) the absorption spectra and (b) the spectral holes after (3) 25, (4) 70, and (5) 180 s after the irradiation.

absorption maximum. The change in the absorption spectrum in the long-wavelength ZPL wing (in the range of its overlap with the laser line) is much larger than in the short-wavelength absorption wing. This fact indicates that the ZPL absorption spectrum selectively changes under laser irradiation. However, the selective change in the line shape is superimposed on the nonselective decrease in absorption; therefore, the spectral hole is weakly pronounced.

The wavelength-selective component of the ZPL absorption spectrum can be found using the method proposed in [24]. It is based on determining the shapes of the individual components of spectral profile if individual bands are present in several measured spectra in different combinations. Let us consider the case where the absorption spectra $K_1(\lambda)$ and $K_2(\lambda)$ consist of two bands, $g_{\text{inh}}(\lambda)$ and $g_{\text{hole}}(\lambda)$, which make contributions with arbitrary coefficients $\alpha_{1,2}$ and $\beta_{1,2}$: $K_1(\lambda) = \alpha_1 g_{\text{inh}}(\lambda) + \beta_1 g_{\text{hole}}(\lambda)$ and $K_2(\lambda) = \alpha_2 g_{\text{inh}}(\lambda) + \beta_2 g_{\text{hole}}(\lambda)$. In our case the first band is the total ZPL absorption profile, while the $g_{\text{hole}}(\lambda)$ band determines the selective component of the spectral change. The $\beta_{1,2}$ values can be, for example, negative, which means subtraction of the $g_{\text{hole}}(\lambda)$ profile from the spectrum formed by the $g_{\text{inh}}(\lambda)$ band. To determine the spectral hole shape, one must solve a system of linear equations.

If one of the profiles is known to be zero at some wavelength [for example, $g_{\text{hole}}(\lambda_0) = 0$], $K_1(\lambda_0)K_2^{-1}(\lambda_0) = \alpha_1/\alpha_2$ and the shape of one of the bands can be found using the relation

$$K_1(\lambda) - K_2(\lambda) \frac{K_1(\lambda_0)}{K_2(\lambda_0)} = \left(\beta_1 - \frac{\alpha_1}{\alpha_2} \beta_2 \right) g_{\text{hole}}. \quad (5)$$

The obtained profile corresponds to the shape of an individual spectral line (spectral hole in our case). The experimental curves were normalised to the wavelength $\lambda_0 = 523$ nm, which is near the short-wavelength edge of the ZPL absorption band and relatively far from the laser excitation wavelength. It is unreasonable to increase even more the spacing between the laser line and absorption peak, because experimental errors and measurement noise become significant in this case. The spectral hole in the experimental curves is shown in Fig. 3b (the laser radiation spectrum and the spectrum of N_1 -CC ZPL are also presented for comparison). It can be seen that the spectral hole amplitude increases with the irradiation time, while the spectral width does not change. In the experiment the width $\Delta\lambda_{\text{hole}} = 0.24$ nm for the selective spectral hole at the total ZPL width $\Delta\lambda_{\text{inh}} = 0.33$ nm. The width of the selective component of the spectral change in the absorption band turned out to be smaller than the width of inhomogeneous profile by a factor of 1.5 (and, in turn, larger than the width of the measured laser line by a factor of 4).

Such a wide spectral hole can be caused, in particular, by fine splitting of N_1 -CC levels within the inhomogeneous profile. The nonselective change in the optical density of entire ZPL occurred at a higher rate than the selective hole burning, which hindered the formation of a deep spectral hole. This behaviour is not typical of neutral and negatively charged CCs, where the ionisation under selective laser irradiation is the main mechanism of CC selective destruction. The ionisation rate in positively charged CCs is much lower; therefore, the weak selective change in ZPL is indicative of positive charge of the aforementioned CC. The main mechanism of nonselective destruction (especially

in the initial stage) is the capture of electron formed as a result of ionisation of CCs of other types (F_2 , F_3^- , F_2^-). It follows from the aforesaid that the homogeneous and inhomogeneous broadenings have the same order of magnitude. As a result, the maximum of the spectral hole burning (Fig. 3b) is shifted with respect to the laser line toward the maximum absorption range.

The change in the F_3^+ -CC ZPL at $\lambda = 488$ nm under selective excitation and $T = 14$ K was investigated in further experiments. The initial ZPL spectra were characterised by the optical density $OD = 0.55$ and FWHM $\Delta\lambda_{\text{inh}} = 0.35$ nm. Figure 4 presents experimental curves (1–4), obtained before and after irradiation at $\lambda = 487.36$ nm. Both selective and nonselective changes in the transmission spectrum are observed. A procedure similar to that described in the previous experiment, with normalisation to $\lambda = 487.36$ nm, was performed to isolate the selective component of change in the spectrum, and the spectra were subtracted after this normalisation [curve (5)]. The selective hole width $\Delta\lambda_{\text{hole}}$ was 0.17 nm in this experiment, which exceeds the measured laser linewidth by a factor of about 2. However, the hole depth remained small and corresponded to $OD = 0.06$, which is smaller than the nonselective change in the ZPL amplitude by a factor of about 5 and lower than the initial optical ZPL density by a factor of 14.

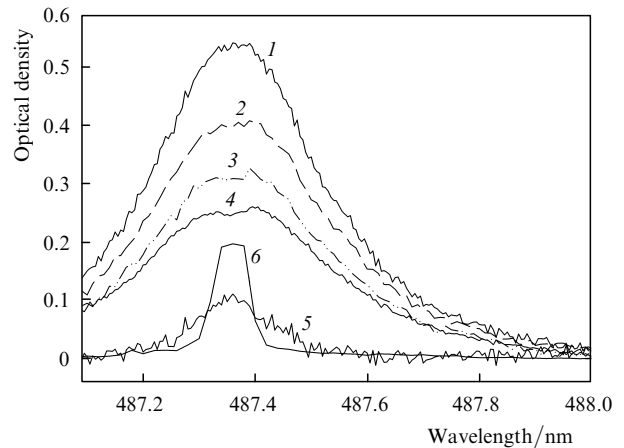


Figure 4. Absorption ZPL spectra at $\lambda = 487.36$ nm: (1) initial spectrum; (2–4) the spectra recorded (2) 3, (3) 16, and (4) 26 min after irradiation; (5) the spectral hole 26 min after irradiation; and (6) the laser radiation spectrum.

Having compared the data on selective hole burning in the F_3^+ - and N_1 -CC ZPLs, we should note that strong nonselective destruction of both centres significantly advances the spectral hole formation. This indicates that the main mechanism of destruction of these CCs is not related to selective absorption of radiation. In our opinion, the key factor is the capture of the electrons formed during ionisation of centres of other types. This process explains the nonselective decrease in the concentration of both CCs, which dominates over the selective hole burning. The absence of deep selective holes in the spectra of F_3^+ and N_1 CCs (in contrast to the holes in the F_2^- - and F_3^- - CCs) suggests that the N_1 CC is positively charged and is most likely to be an isomer of $(F_3^+)^*$ or F_4^+ CCs.

4. Conclusions

We have investigated the absorption ZPL in LiF crystals by the methods of classical and selective laser spectroscopy. The inhomogeneous line broadening was 15 and 11 cm^{-1} for F_3^+ - and N_1 CCs. The homogeneous ZPL broadening dominated at temperatures above 40 and 70 K for F_3^+ - and N_1 CCs, respectively. Within the experimental error the temperature broadening of ZPL can be described in terms of coupling between CC and an optical phonon with a frequency found from the absorption spectrum. The comparison of the temperature broadening and shift of N_1 -CC ZPL made it possible to determine the quadratic electronic–vibrational coupling constant. The widths of the spectral holes burned in ZPLs under laser irradiation at $T = 15$ K were 0.16 and 0.24 nm for F_3^+ and N_1 CCs, respectively. The dominant nonselective mechanism of decreasing the N_1 -CC ZPL amplitude indicates that this CC is positively charged.

Acknowledgements. We are grateful to S.B. Mirov for the possibility of carrying out the experiment and to T.T. Basiev for his interest in this study.

References

1. Moerner W.E., in *Current Physics* (Berlin: Springer, 1988) Vol. 44.
2. Kaplyanskii A.A., Macfarlane R.M., in *Spectroscopy of Solids Containing Rare Earth Ions* (Amsterdam: Elsevier, 1987).
3. Sild O., Haller K., in *Zero-phonon Line and Spectral Hole Burning in Spectroscopy and Photochemistry* (Berlin–Heidelberg: Springer, 1988).
4. Rebane K.K. *J. Luminesc.*, **100**, 219 (2002).
5. Basiev T.T., Mirov S.B., in *Room Temperature Tunable Color Center Lasers* (Chur, Switzerland: Harwood Acad. Publ. GmbH, 1994).
6. Jenkins N.W., Mirov S.B., Fedorov V.V. *J. Luminesc.*, **91**, 147 (2000).
7. Basiev T.T., Papashvili A.G., Fedorov V.V., Vassiliev S.V., Gellermann W. *Laser Phys.*, **14**, 23 (2004).
8. Moerner W.E., Pokrowsky P., Schellenberg F.M., Bjorklund G.C. *Phys. Rev. B*, **33**, 5702 (1986).
9. Fedorov V.V., Mirov S.B., Ashenafi M., Xie L. *Appl. Phys. Lett.*, **79**, 2318 (2001).
10. Kazumata Y. *Phys. Stat. Sol.*, **17**, 131 (1966).
11. Basiev T.T., Mirov S.B., Osiko V.V. *IEEE J. Quantum Electron.*, **24**, 1052 (1988).
12. Feofilov P.P. *The Physical Basis of Polarized Emission* (New York: Consultants Bureau, 1961).
13. Bauman G., von der Osten W., Waidelich W. *Z. Angew. Phys.*, **22**, 246 (1967).
14. Johansson G., von der Osten W., Piehl R., Waidelich W. *Phys. Stat. Sol.*, **34**, 699 (1969).
15. Nahum J. *Phys. Rev.*, **158**, 814 (1967).
16. Blieden G.S., Comins J.D., Derry T.E. *Nucl. Instrum. Meth. Phys. Res. B*, **80**, 1215 (1993).
17. Tsuboi T., Ter-Mikirtychev V.V. *Opt. Commun.*, **116**, 389 (1995).
18. Fitchen D.B., in *Physics of Colour Centers* (New York: Acad. Press, 1968) p. 293.
19. Kaplyanskii A.A., Medvedev V.N., Skvortsov A.P. *Surface Sci.*, **37**, 650 (1973).
20. Osad'ko I.S., in *Spectroscopy and Excitation Dynamics of Condensed Molecular Systems* (Amsterdam: North-Holland, 1983).
21. Hsu D., Skinner J.L. *J. Chem. Phys.*, **88**, 679 (1987).
22. Bickham S.R., Sievers A.J. *Phys. Rev. B*, **43**, 2339 (1991).
23. Hsu D., Skinner J.L. *J. Chem. Phys.*, **81**, 5471 (1984).
24. Fok M.V. *Trudy FIAN*, **59**, 3 (1972).